

# High density polyethylene and zirconium phosphate nanocomposites

Adan Santos Lino<sup>1</sup>, Luis Claudio Mendes<sup>2\*</sup>, Daniela de França da Silva<sup>2</sup> and Olaf Malm<sup>1</sup>

<sup>1</sup>Laboratório de Radioisótopos Eduardo Penna Franca, Instituto de Biofísica Carlos Chagas Filho, Universidade Federal do Rio de Janeiro – UFRJ, Rio de Janeiro, RJ, Brazil

<sup>2</sup>Instituto de Macromoléculas Professora Eloisa Mano, Universidade Federal do Rio de Janeiro – UFRJ, Rio de Janeiro, RJ, Brazil

\*lcmendes@ima.ufrj.br

## Abstract

Nanocomposite based on high density polyethylene (HDPE) and layered zirconium phosphate organically modified with octadecylamine (ZrPOct) was obtained through melt processing. The ZrPOct was synthesized by precipitation and modified by suspension and sonication procedures. The initial and maximum degradation temperatures ( $T_{onset}$  and  $T_{max}$ ) were increased. A slight decrease of crystallinity degree was detected. Reduction of elastic modulus and elongation at break were noticed. The lamellar spacing was increased (3.3 times higher). The storage modulus decreased and low field nuclear magnetic resonance (LFNMR) revealed an increasing of molecular mobility. The presence of octadecylamine enhanced the entrance of HDPE in the ZrPOct galleries. Several characteristics of HDPE were changed indicating that intercalation was successful. All results indicated that partially intercalated and/or exfoliated nanocomposite was achieved.

**Keywords:** *nanocomposite, HDPE, layered zirconium phosphate.*

## 1. Introduction

Over the past two decades great advances in nanotechnology emerged, which is considered a promising technology of the 21<sup>st</sup> century. Great potential for innovations that increase the economic prosperity and sustainable development are expected<sup>[1,2]</sup>. Recent study indicates that nanocomposites occur naturally through synergistic effect as found in nacre (the outer layer of pearls) consisted of proteins, polysaccharides and nanometric layers of calcium carbonate ( $\text{CaCO}_3$ ). To produce advanced materials, researchers are investigating and trying to adjust natural composites to their level of structural control and properties<sup>[3]</sup>. The addition of fillers enhances mechanical, thermal and barrier properties of the composites<sup>[4,5]</sup>. Synthetic nanocomposites have been prepared with various polymers and montmorillonite (MMT) is the most common filler used. In turn, the use of layered zirconium phosphate (ZrP), an inorganic and synthetic filler, in the formation of a nanocomposite results in a material with higher aspect ratio, purity and surface energy advantages in relation to MMT<sup>[6,7]</sup>.

The polyethylene family is diversified. High density polyethylene (HDPE) and linear low density polyethylene (LLDPE) are marked members. Although they are produced by Ziegler-Natta and metallocenic catalyst they are homopolymer and copolymer, respectively. HDPE is a homopolymer obtained by coordination polymerization of ethylene gas. Its polymeric chains are linear and constituted by the catenation of ethylene mers. LLDPE is a copolymer obtained by coordination polymerization of ethylene gas with an alpha-olefin (propylene, butane, hexane, etc). It is considered a branched polymer once its polymeric chains are constituted by mers of ethylene and mers of alpha-olefin (propylene is commercially more common). As a consequence

of those branching in LLDPE, its properties differ a lot from those presented by HDPE. For instance, the density, degree of crystallinity, melting temperature and Young's modulus are quite different<sup>[8]</sup>. High-density polyethylene (HDPE) is a semicrystalline polymer with many advantages – low density, strong tenacity, high resistance to impact, abrasion and corrosion. Additionally, inertia to the majority of chemicals, low toxicity and long lifetime contribute for large industrial applications<sup>[9]</sup>. Nanoparticles of silicalite-1 were used with HDPE. Rheological and physical properties were investigated. The authors observed slight effect on the melting temperature, onset degradation temperature and decreasing of intensity of HDPE diffraction peaks<sup>[10]</sup>. It was found that ultrasonic treatment enhanced the intercalation of HDPE into lattice layers of clay by increasing d-spacing up to 50%<sup>[11]</sup>. Impact strength, modulus, and flexural strength of HDPE/exfoliated graphite nanocomposites were compared to others types of reinforcement (glass fibers and carbon black). Polymer nanocomposites from HDPE/exfoliated graphite were equivalent in flexural stiffness and strength to HDPE composites reinforced with glass fibers and carbon black<sup>[12]</sup>. Synergistic effect introduced by nanoparticles of nano- $\text{CaCO}_3$  and OMMT in HDPE was reported<sup>[13,14]</sup> inferred that a higher degree of exfoliation for nanosized clay particles is key to enhancing the rheological, mechanical, and flame retarding properties even when small amounts of clay (less than 1%) are used.

Considering that it was not found scientific article related to nanocomposite of HDPE and zirconium phosphate modified with long-chain amine, the aim of this work was to investigate the influence of the intercalation of octadecylamine inside ZrP galleries on the HDPE characteristics. Through

thermal, crystallographic, thermo-mechanical, tensile and molecular mobility analyses the formation of intercalated and/or exfoliated nanocomposite was evaluated.

## 2. Materials and Methods

### 2.1 Materials

High-density polyethylene (HDPE) – melt flow index of 0.35 g/10 min and density of 0.960 g/cm<sup>3</sup> – was provided by Braskem (Triunfo, RS, Brazil). Phosphoric acid, zirconium oxychloride and octadecylamine were purchased (Aldrich Co.).

### 2.2 Synthesis of layered zirconium phosphate

The ZrP was synthesized by direct precipitation method<sup>[15]</sup>. An 12M phosphoric acid solution (H<sub>3</sub>PO<sub>4</sub>) and zirconium oxychloride were mixed in the proportion of P/Zr = 18. The system was kept under agitation and reflux at 110 °C, for 24 hours. After that, the resulting material was centrifuged (3400 rpm for 30 min) and washed successively with deionized water in order to obtain neutral pH and absence of chloride<sup>[16-18]</sup>. The resulting solid was placed in a freezer at –80 °C for 24 hours and then submitted to lyophilization for 4 days.

### 2.3 Modification of the layered zirconium phosphate

The ZrP was modified by intercalation of amine according to the experimental procedure<sup>[19,20]</sup>. A certain amount of  $\alpha$ -ZrP and a solution of octadecylamine (2:1 alcohol/water) were mixed at an amine/ $\alpha$ -ZrP molar ratio of 1.5. The product was centrifuged and washed successively with alcohol to remove the excess of amine. As before, the resulting solid was placed in a freezer at –80 °C for 24 hours and then submitted to lyophilization for 4 days. The final product was labeled as ZrPOct.

### 2.4 Preparation of nanocomposites

Nanocomposites of HDPE and layered zirconium phosphates – neat and organically modified with octadecylamine – with a fixed phosphate percentage of 2% w/w, were processed in a counter-rotating twin-screw extruder. The extruder was adjusted to operate at 100 rpm and temperature profile of 160 °C (input) and 170 °C, 180 °C and 190 °C (output), conditions recommended by the polymer manufacturer. The extrudate was cooled and granulated. In order to homogenize the nanocomposite, the material was reprocessed under the same conditions. In order to characterize the material, thin plates was processed in Carver press at 210 °C, with load of 5000 kg for 7 minutes.

## 2.5 Characterization

### 2.5.1 Low field nuclear resonance magnetic (LFNMR)

The relaxation time of the HDPE and nanocomposites, <sup>1</sup>H low-field nuclear magnetic resonance (<sup>1</sup>HLFNMR) analysis was carried out in a Maran Ultra 23 low-field NMR device. The relaxation time (T<sub>1</sub>) was measured in time intervals of 10 seconds and 20 points, at 27 °C. The result was expressed in terms of domain curves.

### 2.5.2 Dynamic-mechanical analysis (DMA)

Dynamic-mechanical analysis (DMA) was carried out in a TA Instruments Q800 instrument, using rectangular specimens with dimensions of 8x 1x 0.1 cm, scanning from –150 to 100 °C, heating rate of 2 °C/min and frequency of 1 Hz, in the single-cantilever mode. The storage modulus (E'), the loss modulus (E'') and loss tangent (tan $\delta$ ) were determined.

### 2.5.3 Wide angle X-ray diffraction (WAXD)

The WAXD was performed in a Rigaku Miniflex diffractometer, employing CuK $\alpha$  radiation with wavelength of 1.5418Å and Ni filter, at a voltage of 30kV and current of 15mA, with 2 $\theta$  between 2-35°. From the diffractograms it was identified the crystallographic planes and calculated the interlamellar spacing, using Bragg's equation.

### 2.5.4 Thermogravimetry (TGA)

The thermal stability was evaluated in a TA Instruments Q500 thermogravimetric analyzer. The thermogravimetric curves were obtained between 30 and 700 °C, at 10 °C/min, under a nitrogen atmosphere. The temperatures of initial, maximum and final degradation (T<sub>INICIAL</sub>, T<sub>MAX</sub> and T<sub>FINAL</sub>) were determined as well the residue.

### 2.5.5 Differential scanning calorimetry (DSC)

The calorimetric properties were proceeded using a TA Instruments Q1000 differential scanning calorimeter (DSC). Three thermal cycles were applied. At first, the sample was heated from 40 to 200 °C at 10 °C/min under a nitrogen atmosphere and then kept for 2 minutes in order to eliminate the thermal history. Following, it was cooled to 40 °C at 10 °C/min. Finally, a second heating cycle was carried out under the same conditions as the first. The melting temperature (T<sub>m</sub>) was measured considering the curve plotted from the second heating cycle. The crystallization temperature (T<sub>c</sub>) was determined when possible. The melting enthalpy ( $\Delta H_m$ ) was used to calculate the crystallinity degree (X<sub>c</sub>), considering the melting enthalpy of the 100% crystalline HDPE (290 J.g<sup>-1</sup>) and corrected regarding the HDPE content.

### 2.5.6 Tensile measurements

Stress-strain test was performed by using an Instron model 5569 universal testing system, according to the ASTM D 638 with a 10-kN load cell and testing velocity of 10 mm/min. The parameters assessed were the elastic modulus, stress and elongation at break and stress and elongation at yield. The results were expressed considering the mean of five test specimens.

### 2.5.7 Flowability

The effect of the zirconium phosphate nanoparticles on the HDPE melt flow rate (MFR) was analyzed using a Dynisco plastometer following the ASTM D 1238, at 190 °C, 2.16 kg and melt time of 240 seconds.

## 3. Results and Discussions

### 3.1 Hydrogen low field nuclear magnetic resonance

Hydrogen NMR allows obtaining information on sample organization, heterogeneity and particle dispersion. The relaxation data are important to understand the changes in

the molecular structural organization and molecular dynamic of nanocomposites. Solid-state  $^1\text{H}$ NMR spectroscopy is sensitive enough to assess the different chain mobilities in polyethylene<sup>[21]</sup>. Semicrystalline polyethylene is composed of domains with widely different polymer chain mobilities. In the crystalline domain, the chains are highly ordered and can only be reoriented very slowly. In contrast, in noncrystalline domains the polymer chains have high mobility. Table 1 shows the  $T_1\rho$  values and the respective % of domain for the samples. For all the materials, it was not observed notorious displacement of peaks. Figure 1 shows the domain curves of the HDPE and composites. The relaxation curve of the HDPE revealed two domains. At relaxation times shorter than 400,000 s, one of them appeared, attributed to the chain mobility in the amorphous phase, while a second peak was detected at higher relaxation times concerning the rigid region – amorphous chains constricted among HDPE lamellae and crystalline phase – the latter normally being responsible for controlling relaxation process. The absence of relaxation times related to the filler in the composite domain curves is an important indication that good dispersion and filler/polymer interaction has occurred, according to Tavares et al.<sup>[22]</sup> and Mendes et al.<sup>[23]</sup>.

### 3.2 Dynamic-mechanical test

The  $\tan\delta$  curves (Figure 2) and Table 2 showed that the addition of ZrP – modified or not – promoted no influence in glass transition temperature ( $T_g$ ) of the polymer. It was also observed a decrease in storage and loss modulus. Octadecylamine or stearylamine [ $\text{CH}_3-(\text{CH}_2)_{17}-\text{NH}_2$ ] is a long chain amine produced from the chemical reduction of stearic acid. Its chemical structure possesses a hydrocarbon chain with seventeen methylene groups. The HDPE polymer chain is constituted by catenation of thousands ethylene groups (two consecutive methylene groups bonded). The presence of methylene groups in the chemical structure of both should provide strong interaction between HDPE and octadecylamine. It is worth to explain the role of the octadecylamine as modifier of the zirconium phosphate (ZrP) structure. The ZrP is a lamellar crystalline inorganic material which has poor interaction with polymers (organic material). For improving the interaction of ZrP with polyolefins its lamellar structure was organically modified with octadecylamine through acid/base reaction. The presence of octadecylamine between the galleries of ZrP resulted in the lamellae separation – d-spacing of ZrP was increased – and enhanced its organophilic characteristics. Such chemical modification facilitates the entrance of HDPE chains inside of the ZrPOct galleries. Due to the chemical structural similarity with HDPE chains the octadecylamine played a role as plasticizing for polyolefin resulting in decreasing of HDPE storage modulus ( $E'$ ).

### 3.3 WAXD

Figures 3, 4 and 5 show the diffractograms and Table 3 presents diffraction angle and d-spacing of the materials. HDPE diffraction angles occurred at  $2\theta=22.21^\circ$  and  $2\theta=24.52^\circ$  as reported in literature<sup>[24]</sup>. The diffraction angle equivalent to basal spacing of the ZrP occurred at  $2\theta=12^\circ$  with an interlamellar distance of 7.32 Å. In HDPE/ZrP, the diffraction angle of ZrP remained constant but the

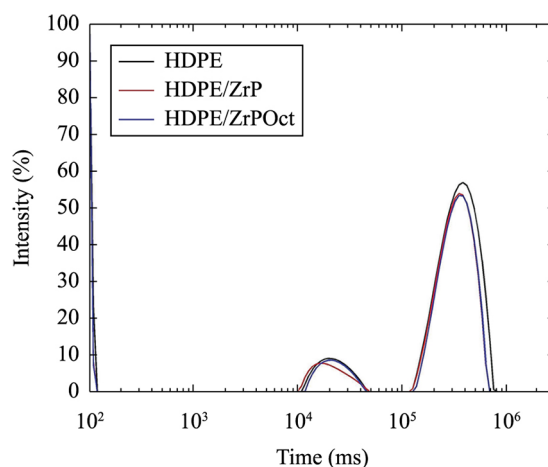


Figure 1.  $^1\text{H}$ LFNMR domain curves of HDPE and composites.

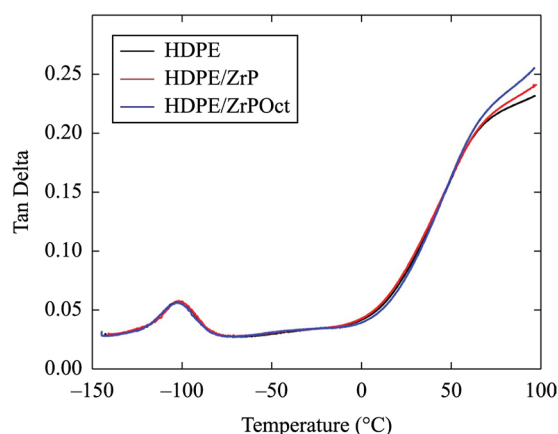


Figure 2. Tan Delta curves of the materials.

Table 1. NMR data of HDPE and composites.

Sample	$T_1\rho$ (ms)	$T_1\rho$ Domain (%)
HDPE	19.68	12.46
	388.13	87.54
HDPE/ZrP	16.60	12.50
	356.43	87.50
HDPE/ZrPOct	21.43	13.00
	356.43	87.00

Table 2. DMA data of HDPE and composites.

Sample	HDPE	HDPE/ZrP	HDPE/ZrPOct
$T_g$ ( $^\circ\text{C}$ )	-102	-102	-102
Loss Modulus ( $E''$ ) at $T_g$ point (MPa)	267	235	219
Storage Modulus ( $E'$ ) at $T_g$ point (MPa)	4690	4104	3915
Tan $\delta$	0.057	0.057	0.056

interlamellar spacing decreased ( $d=7.25$  Å) attributed to loss of water in the interlamellar layer by Costantino et al.<sup>[6]</sup>. In the presence of HDPE, the diffraction angle of ZrPOct decreased from 4.1 to 3.9 $^\circ$  while the interlamellar spacing increased from 21.55 to 23.88 Å. It was also observed a slight shift of the HDPE diffraction planes to small angles

(from 22.21 to 21.7° and 24.52 to 23.9°. The changes could be attributed to the intercalation of the HDPE along the ZrPOct interlamellar layers. It can deduce that partially intercalated and/or exfoliated nanocomposite was achieved.

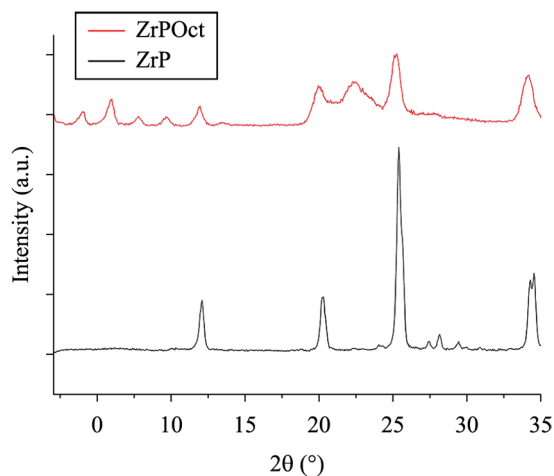


Figure 3. WAXD diffractograms of the ZrP and ZrPOct fillers.

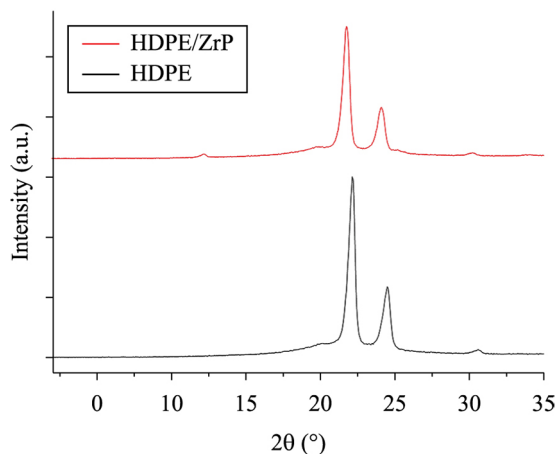


Figure 4. WAXD diffractograms of the HDPE and composite HDPE/ZrP.

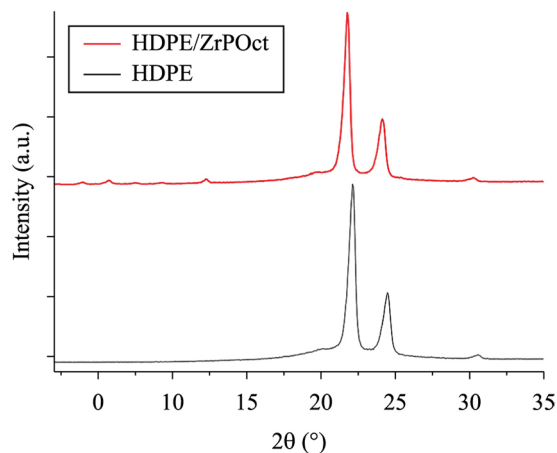


Figure 5. WAXD diffractograms of the HDPE and composite HDPE/ZrPOct.

### 3.4 Thermogravimetry

Table 4 shows the TGA data of the materials. The  $T_{ONSET}$ ,  $T_{MAX}$  and  $T_{FINAL}$  of HDPE and HDPE/ZrP were very similar indicating that a microcomposite was produced. It is currently disseminate that the increasing of thermal stability in polymeric nanocomposites is attributed to layered filler. The lamellae – intercalated or exfoliated – act as barrier to the release of volatile products during degradation<sup>[15,25]</sup>. All thermal properties were higher for HDPE/ZrPOct indicating that a partially and/or exfoliated nanocomposite was produced.

### 3.5 Differential scanning calorimetry

The calorimetric data in Table 5 showed that  $T_c$ ,  $T_m$  and  $X_c$  of HDPE and HDPE/ZrP were very close.  $T_m$  and  $X_c$  of HDPE/ZrPOct attained values slightly lower. Particularly, the HDPE degree of crystallinity was reduced as function of octadecylamine linked into the phosphate lamellae. As mentioned, the amine acted as plasticizing agent of HDPE chain and retarded its crystallization process. It is again evidenced that partially and/or exfoliated nanocomposite was achieved.

### 3.6 Mechanical measurements

Mechanical properties are arranged in Table 6. The elastic modulus increased for HDPE/ZrP and a decreasing was observed for HDPE/ZrPOct. The filler was responsible for decreasing of modulus and also the slight increasing of elongation at break as compared to HDPE/ZrP. The decrease of the Young modulus of the produced nanocomposite probably is also associated to the lower degree of crystallinity, as observed in DSC analysis. Then, it is valid to deduce that a partially and/or exfoliated nanocomposite was produced for HDPE/ZrOct. A decreasing of stress and elongation at break was presented for HDPE/ZrP and HDPE/ZrPOct. Two types of material were produced as function of the type of filler. In the HDPE/ZrP, the ZrP acted as reinforcement of HDPE and it is deduced that a microcomposite was achieved<sup>[26]</sup>.

Table 3.  $2\theta$  values and interlayer distances of the materials.

Sample	$2\theta$ (degrees)	$d_{001}$ (Å)
ZrP	12.00	7.32
HDPE/ZrP	12.17	7.25
ZrPOct	4.10	21.55
HDPE/ZrPOct	3.90	23.88

Table 4. TGA data of the materials.

Sample	$T_{onset}$ (°C)	$T_{max}$ (°C)	$T_{final}$ (°C)	Residue (%)
HDPE	261	453	473	4.7
HDPE/ZrP	270	453	473	3.1
HDPE/ZrPOct	306	470	486	3.1

Table 5. Calorimetric properties of the materials.

Sample	$T_c$ (°C)	$T_m$ (°C)	$\Delta H_a$ (J/g)	$X_c$ (%)
HDPE	115	134	208	72
HDPE/ZrP	116	134	208	72
HDPE/ZrPOct	116	133	201	69

$T_c$  = crystallization temperature;  $T_m$  = melting temperature in the 2<sup>nd</sup> heating;  $\Delta H_a$  = melting enthalpy;  $X_c$  = degree of crystallinity.



**Table 6.** Mechanical properties of the materials.

Property/Sample	HDPE	HDPE/ZrP	HDPE/ZrPOct
Elongation at break (%)	1043±224	216±82	393±81
Stress at break (MPa)	17.5±0.7	14.5±0.9	15.4±2.2
Elastic modulus (MPa)	672±33	733±19	623±28
Elongation at yield (%)	13.8±0.25	12.6±0.60	14.4±0.70
Stress at yield (MPa)	25.6±0.1	25.5±0.3	26.0±0.7

**Table 7.** MFR of the materials.

Sample	MFR (g/10min)
HDPE	0.33±0.03
HDPE/ZrP	0.28±0.02
HDPE/ZrPOct	0.27±0.02

For HDPE/ZrPOct the octadecylamine inside of ZrPOct developed a role as plasticizing agent of HDPE. It was responsible for decreasing of modulus and also the slight increasing of elongation at break as compared to HDPE/ZrP. Then, it is valid to deduce that a partially and/or exfoliated nanocomposite was produced for HDPE/ ZrPOct.

### 3.7 Melt flow rate

MFR values are presented in Table 7. The MFR showed tendency to decrease for HDPE/ZrP and HDPE/ZrPOct. Similar to happen in microcomposites, the fillers provide resistance to flowability of HDPE<sup>[27]</sup>. The lowest value was found to HDPE/ZrPOct due to the entrance of HDPE chain inside de ZrPOct lamellae. It induced to suppose that a partially and/or exfoliated nanocomposite was reached. The findings corroborated to those in WAXD and mechanical measurements.

## 4. Conclusions

Alpha-zirconium phosphate was synthesized and modified with octadecylamine in order to produce nanocomposite based on HDPE. According to some conventional characterization techniques of polymers (DSC, TGA, WAXD, MFR, tensile-deformation) HDPE/ZrP behave as a microcomposite. On the contrary, presence of octadecylamine as intercalation agent of ZrP allowed the increasing of its interlamellar spacing. Also facilitate the entrance of the HDPE chain along the filler galleries. This produced changes in the HDPE behavior. Decreasing of the (d001) diffraction angle, elastic modulus, degree of crystallinity besides increasing of the interlamellar spacing and thermal stability lead to induce that a partially and/or exfoliated nanocomposite was reached.

## 5. Acknowledgements

This work was supported by the Conselho Nacional de Desenvolvimento Científico e Tecnológico (CNPq), Fundação Coordenação de Aperfeiçoamento de Pessoal de Nível Superior (CAPES) e Universidade Federal do Rio de Janeiro (UFRJ). We thank the Instituto de Radioisótopos da UFRJ for drying the lamellar phosphates.

## 6. References

- Hussain, F., Hojjati, M., Okamoto, M., & Gorga, R. E. (2006). Review article: polymer-matrix nanocomposites, processing, manufacturing, and applicatio: an overview. *Journal of Composite Materials*, 40(17), 1511-1575. <http://dx.doi.org/10.1177/0021998306067321>.
- Brito, G. F., Oliveira, A. D., Araújo, E. M., Melo, T. J. A., Barbosa, R., & Ito, E. N. (2008). Nanocompósitos de polietileno/ argila bentonita nacional: influência da argila e do agente compatibilizante PE-g-MA nas propriedades mecânicas e de inflamabilidade. *Polímeros: Ciência e Tecnologia*, 18(2), 170-177. <http://dx.doi.org/10.1590/S0104-14282008000200015>.
- Esteves, A. C. C., Barros-Timmons, A., & Trindade, T. (2004). Nanocompósitos de matriz polimérica: estratégias de síntese de materiais híbridos. *Química Nova*, 27(5), 798-806. <http://dx.doi.org/10.1590/S0100-40422004000500020>.
- Barbosa, R., Araújo, E. M., Melo, T. J. A., & Ito, E. N. (2007). Preparação de argilas organofílicas e desenvolvimento de nanocompósitos de polietileno. Parte 2: comportamento de inflamabilidade. *Polímeros: Ciência e Tecnologia*, 17(2), 104-112. <http://dx.doi.org/10.1590/S0104-14282007000200009>.
- Komatsu, D., Otaguro, H., & Ruvolo Filho, A. C. (2014). Avaliação comparativa entre os nanocompósitos de argila motmorilonita/LLDPE e com hexaniobato de potássio/LLDPE: caracterização das propriedades mecânicas e de transporte. *Polímeros: Ciência e Tecnologia*, 24(1), 37-44. <http://dx.doi.org/10.4322/polimeros.2013.052>.
- Costantino, U., Vivani, R., Zima, V., & Cernoskova, E. (1997). Thermoanalytical study, phase transitions, and dimensional changes of  $\alpha$ -Zr(HPO<sub>4</sub>)<sub>2</sub>·H<sub>2</sub>O large crystals. *Journal of Solid State Chemistry*, 132(1), 17-23. <http://dx.doi.org/10.1006/jssc.1997.7385>.
- Sue, H. J., Gam, K. T., Bestaoui, N., Spurr, N., & Clearfield, A. (2004). Epoxy nanocomposites based on the synthetic  $\alpha$ -zirconium phosphate layer structure. *Chemistry of Materials*, 16(2), 242-249. <http://dx.doi.org/10.1021/cm030441s>.
- Chum, P. S., & Swogger, K. (2008). Olefin polymer technologies: history and recent progress at The Dow Chemical Company. *Progress in Polymer Science*, 33(8), 797-819. <http://dx.doi.org/10.1016/j.progpolymsci.2008.05.003>.
- Chrissafis, K., Paraskevopoulos, K. M., Pavlidou, E., & Bikiaris, D. (2009). Thermal degradation mechanism of HDPE nanocomposites containing fumed silica nanoparticles. *Thermochimica Acta*, 485(1-2), 65-71. <http://dx.doi.org/10.1016/j.tca.2008.12.011>.
- Chae, D. W., Kim, K. J., & Kim, B. C. (2006). Effects of silicate-1 nanoparticles on rheological and physical properties of HDPE. *Polymer*, 47(10), 3609-3615. <http://dx.doi.org/10.1016/j.polymer.2006.03.053>.
- Swain, S. K., & Isayev, A. I. (2007). Effect of ultrasound on HDPE/clay nanocomposites: Rheology, structure and properties. *Polymer*, 48(1), 281-289. <http://dx.doi.org/10.1016/j.polymer.2006.11.002>.
- Jiang, X., & Drzal, L. T. (2010). Multifunctional high density polyethylene nanocomposites produced by incorporation of exfoliated graphite nanoplatelets 1: morphology and mechanical properties. *Polymer Composites*, 31(6), 1091-1098. <http://dx.doi.org/10.1002/pc.20896>.
- Dai, X., Shang, Q., Jia, Q., Li, S., & Xiu, Y. (2010). Preparation and properties of HDPE/CaCO<sub>3</sub>/OMMT ternary nanocomposite. *Polymer Engineering and Science*, 50(5), 894-899. <http://dx.doi.org/10.1002/pen.21608>.
- Lee, Y. H., Park, C., Sain, M., Kontopoulou, M., & Zheng, W. (2007). Effects of clay dispersion and content on the rheological, mechanical properties, and flame retardance of HDPE/clay

- nanocomposites. *Journal of Applied Polymer Science*, 105(4), 1993-1999. <http://dx.doi.org/10.1002/app.26403>.
15. Alberti, G., Costantino, U., Allulli, S., & Tomassini, N. (1978). Crystalline  $Zr(R-PO_3)_2$  and  $Zr(R-OPO_3)_2$  compounds: a new class of materials having layered structure of the zirconium phosphate type. *Journal of Inorganic and Nuclear Chemistry*, 40(6), 1113-1117. [http://dx.doi.org/10.1016/0022-1902\(78\)80520-X](http://dx.doi.org/10.1016/0022-1902(78)80520-X).
16. Clearfield, A., & Smith, G. D. (1969). The crystallography and structure of zirconium bis(monohydrogen orthophosphate) monohydrate. *Inorganic Chemistry*, 8(3), 431-436. <http://dx.doi.org/10.1021/ic50073a005>.
17. Brandão, L. S., Mendes, L. C., Medeiros, M. E., Sirelli, L., & Dias, M. L. (2006). Thermal and mechanical properties of poly(ethylene terephthalate)/lamellar zirconium phosphate nanocomposites. *Journal of Applied Polymer Science*, 102(4), 3868-3876. <http://dx.doi.org/10.1002/app.24096>.
18. Ramis, L. B. (2007). *Compósitos termoplásticos contendo fosfatos e fosfonatos lamelares de zircônio e titânio* (Master's thesis). Instituto de Macromoléculas Professora Eloisa Mano, Universidade Federal do Rio de Janeiro, Rio de Janeiro.
19. Pérez-Santano, A., Trujillano, R., Belver, C., Gil, A., & Vicente, M. A. (2005). Effect on the intercalation conditions of a montmorillonite with octadecylamine. *Journal of Colloid and Interface Science*, 284(1), 239-244. <http://dx.doi.org/10.1016/j.jcis.2004.09.066>. PMID:15752808.
20. Weiss, Z., Valaskova, M., Kristkova, M., Capkova, P., & Pospisil, M. (2003). Intercalation and grafting of vermiculite with octadecylamine using low-temperature melting. *Clays and Clay Minerals*, 51(5), 555-565. <http://dx.doi.org/10.1346/CCMN.2003.0510509>.
21. Eckman, R. R., Henrichs, P. M., & Peacock, A. J. (1997). Study of polyethylene by solid state NMR relaxation and spin diffusion. *Macromolecules*, 30(8), 2474-2481. <http://dx.doi.org/10.1021/ma9516753>.
22. Tavares, M. I. B., Rodrigues, T., Soares, I., Moreira, A., & Ferreira, A. (2009). The use of solid state NMR to characterize high density polyethylene/organoclay nanocomposites. *Chemistry and Chemical Technology*, 3(3), 187-190. Retrieved in 12 December 2014, from <http://old.lp.edu.ua/fileadmin/ICCT/journal/Vol.3/Num.3/05.pdf>
23. Mendes, L. C., Silva, D. F., & Lino, A. S. (2012). Linear low-density polyethylene and zirconium phosphate nanocomposites: evidence from thermal, thermo-mechanical, morphological and low-field nuclear magnetic resonance techniques. *Journal of Nanoscience and Nanotechnology*, 12(12), 8867-8873. <http://dx.doi.org/10.1166/jnn.2012.6718>. PMID:23447930.
24. Cestari, S. P. (2010). *Papel sintético sustentável para embalagem* (Master's thesis). Instituto de Macromoléculas Professora Eloisa Mano, Universidade Federal do Rio de Janeiro, Rio de Janeiro.
25. Ray, S. S., & Okamoto, M. (2003). Polymer/layered silicate nanocomposites: a review from preparation to processing. *Progress in Polymer Science*, 28(11), 1539-1641. <http://dx.doi.org/10.1016/j.progpolymsci.2003.08.002>.
26. Alexandre, M., & Dubois, P. (2000). Polymer-layered silicate nanocomposites: preparation, properties and uses of a new class of materials. *Materials Science and Engineering*, 28(1-2), 1-63. [http://dx.doi.org/10.1016/S0927-796X\(00\)00012-7](http://dx.doi.org/10.1016/S0927-796X(00)00012-7).
27. Rocha, M. C. G., Coutinho, F. M. B., & Estephen, B. (1994). Índice de fluidez: uma variável de controle de processos de degradação controlada de polipropileno por extrusão reativa. *Polímeros: Ciência e Tecnologia*, 4(3), 33-37. Retrieved in 12 December 2014, from <http://www.revistapolimeros.org.br/PDF/v4n3/v4n3a03.pdf>

Received: Dec. 12, 2014

Revised: Apr. 08, 2015

Accepted: July 07, 2015